Acta Chemica Scandinavica, 1993: 47: 368–373
Printed in Belgium – all rights reserved

ACTA
CHEMICA SCANDINAVICA
ISSN 0904–213X

Molecular Structure of Pentamethylantimony by Gas Electron Diffraction; Structure and Bonding in $Sb(CH_3)_5$ and $Bi(CH_3)_5$ Studied by *Ab Initio* MO Calculations

Arne Haaland,[a,*] Andreas Hammel,[a] Kristin Rypdal,[a] Ole Swang,[a] Jon Brunvoll,[b] Odd Gropen,[c] Michael Greune[d] and Johann Weidlein[d]

[a]Department of Chemistry, University of Oslo, Box 1033 Blindern, N-0315 Oslo, Norway, [b]Institute of Theoretical Chemistry, University of Trondheim NTH, N-7034 Trondheim, Norway, [c]Department of Chemistry, Institute of Mathematical and Physical Sciences, University of Tromsø, N-9001 Tromsø, Norway and [d]Institute of Inorganic Chemistry, University of Stuttgart, Pfaffenwaldring 55, D-7000 Stuttgart 90, Germany

Haaland, A., Hammel, A., Rypdal, K., Swang, O., Brunvoll, J., Gropen, O., Greune, M. and Weidlein, J., 1993. Pentamethylantimony; Structure and Bonding Studied by Gas Electron Diffraction and *Ab Initio* MO Calculations. – Acta Chem. Scand. 47: 368–373.

The electron diffraction pattern of $Sb(CH_3)_5$ recorded with an all-glass inlet system at room temperature confirms the trigonal bipyramidal structure and yields the bond distances Sb–C_{eq} = 214.0(5) pm and Sb–C_{ax} = 226.4(11) pm. ^{13}C NMR spectra in CD_2Cl_2 contain only one line which remains sharp down to −90°C. The molecule presumably undergoes Berry pseudorotation over a square pyramidal transition state which leads to rapid exchange of axial and equatorial methyl groups. Trigonal bipyramidal and square pyramidal models of $Sb(CH_3)_5$ were optimized at the SCF MO level. Electron correlation was included with the modified coupled pair functional (MCPF) method. The calculations at this level suggest that the energy of the trigonal bipyramidal configuration is 7.1 kJ mol^{-1} below the energy of the square pyramidal configuration. Similar calculations on the unknown compound $Bi(CH_3)_5$ suggest that this molecule too would have an trigonal bipyramidal equilibrium configuration.

The molecular structures of pentaphenylphosphorus, PPh_5, and pentaphenylarsenic, $AsPh_5$, are trigonal bipyramidal in the crystalline phase,[1,2] while the molecular structures of the antimony and bismuth analogs, $SbPh_5$ and $BiPh_5$, are square pyramidal.[3,4]

When $SbPh_5$ is crystallized with 0.5 mol cyclohexane, the structure is trigonal bipyramidal,[5] and so is the structure of crystalline penta-*p*-tolylantimony:[6] the energy difference between the two configurations is clearly so small that the structure adopted in the crystalline phase is determined by intermolecular forces.

^{13}C NMR spectra of $SbPh_5$ at room temperature show that the rings are magnetically equivalent,[7] and ^1H NMR spectra of $SbPh_5$ which is fully deuterated in the *meta* and *para* positions show only one line (due to *ortho* protons) down to −142°C.[7] Thus NMR spectroscopy gives no information about the equilibrium configuration in solution. If the equilibrium structure is trigonal bipyramidal, rapid exchange of axial and equatorial ligands may proceed by Berry pseudorotation.[8]

The metal atom and one of the equatorial carbon atoms, often referred to as 'pivotal', remain essentially at rest while the angle subtended by the two other equatorial carbon atoms, $\angle C_{eq}SbC_{eq}$, increases from 120 to 180° and the angle formed by the two axial C atoms, $\angle C_{ax}SbC_{ax}$, decreases from 180 to 120° in a concerted fashion. The initial and final configurations share a twofold symmetry axis, and two symmetry planes intersecting each other along the pivotal Sb–C bond. These symmetry elements are assumed to be preserved during the exchange process, and the transition state is assumed to have C_{4v} symmetry.

Conversely, if the equilibrium configuration is square pyramidal, exchange of apical and basal carbon atoms may proceed through a transition state of near D_{3h} symmetry. The NMR spectra are thus consistent with the conclusion that the energy difference between the two configurations is small.

^1H and ^{13}C NMR spectra of penta-*p*-tolyl antimony in $CHFCl_2$ solution showed that the molecule remained fluxional down to −130°C, hence the equilibrium conformation could not be established, but line shape analysis of ^1H and ^{13}C spectra yielded activation energies of 6.7 and 6.1 kJ mol^{-1}, respectively.[9]

Several derivatives of pentaphenylbismuth have been synthesized, and eight of them have been characterized by X-ray crystallography by Seppelt and coworkers.[10–12] The majority form square pyramids: only one is found to form a trigonal bipyramid. The crystals with square pyramidal

* To whom correspondence should be addressed.

molecules exhibit strong colors: electronic spectra indicate that both configurations are present in solution.[13]

Much less is known about pentaalkyl derivatives of the Group 15 elements. The synthesis of pentamethylantimony was first reported by Wittig and Torsell in 1953;[14] the synthesis of pentamethylarsenic by Mitschke and Schmidbaur in 1973.[15] The phosphorus and bismuth analogs are unknown. Infrared and Raman spectra of neat $As(CH_3)_5$ and $Sb(CH_3)_5$ provide strong evidence for MC_5 frames of D_{3h} symmetry.[15,16]

^1H NMR spectra of $Sb(CH_3)_5$ in CS_2 solution[17] and of $As(CH_3)_5$ in [$^2H_8$]-toluene[15] consist of one narrow line down to -100 and -95°C, respectively. The mechanism of exchange of equatorial and axial methyl groups is unknown, but it is assumed to proceed intramolecularly via Berry pseudorotation.

In this article we report the determination of the molecular structure of $Sb(CH_3)_5$ by gas electron diffraction. We also report the ^{13}C NMR spectrum of $Sb(CH_3)_5$ down to -90°C, and discuss the structure and bonding based on the results of MO calculations at different levels. Finally we report the results of similar calculations on $Bi(CH_3)_5$ which indicate that the equilibrium configuration is trigonal bipyramidal like $Sb(CH_3)_5$.

Experimental

Synthesis. $(CH_3)_3SbCl_2$ was synthesized from $Sb(CH_3)_3$ and Cl_2.[18] Reaction with stoichiometric amounts of $LiCH_3$ in ether yielded $Sb(CH_3)_5$, which was purified by distillation.[14] The yield with respect to $Sb(CH_3)_3$ was 75–80%.

^{13}C-NMR spectra. Spectra were recorded at 75.429 MHz in CD_2Cl_2 solution at 20, 0 and -90°C. All spectra exhibited one peak for the methyl C atoms. The frequency changed slightly with temperature: 14.85 ppm at 20°C, 14.20 ppm at 0°C and 13.43 ppm at -90°C. The linewidth at -90°C was only 1.6 Hz, compared with 6.3 Hz at 0°C and 8.2 Hz at 20°C.

Gas electron diffraction. A few years ago we attempted to record the gas electron diffraction pattern of $Sb(CH_3)_5$ with a stainless-steel inlet system, but found the sample to undergo partial decomposition, presumably to $Sb(CH_3)_3$ and ethane. This time we used an all-glass inlet system to a Balzers Eldigraph KDG2[19] with the nozzle at 20 ± 3°C. Exposures were made with nozzle-to-plate distances of about 50 and 25 cm. Optical densities of were recorded on our Snoopy densitometer and processed by standard procedures.[20] Atomic scattering factors were taken from Ref. 21. Backgrounds were drawn as fourth-degree (50 cm) and sixth-degree (25 cm) polynomials to the difference between total experimental and calculated molecular intensity curves. Comparison of modified molecular intensity curves obtained from single photographic plates showed that while the curves obtained from 50 cm plates were consistent, the curves obtained from 25 cm plates appeared to be plagued by an unusually high noise level. The experiment was repeated, but the quality of the 25 cm data was not improved. This study is based on the best six plates obtained for each nozzle-to-plate distance. The final modified molecular intensity curves extending from $s = 13.75$ to 145.00 nm^{-1} with increment 1.25 nm^{-1} (50 cm) and from $s = 35.00$ to 200.00 nm^{-1} with increment 2.50 nm^{-1} (25 cm) are displayed in Fig. 1.

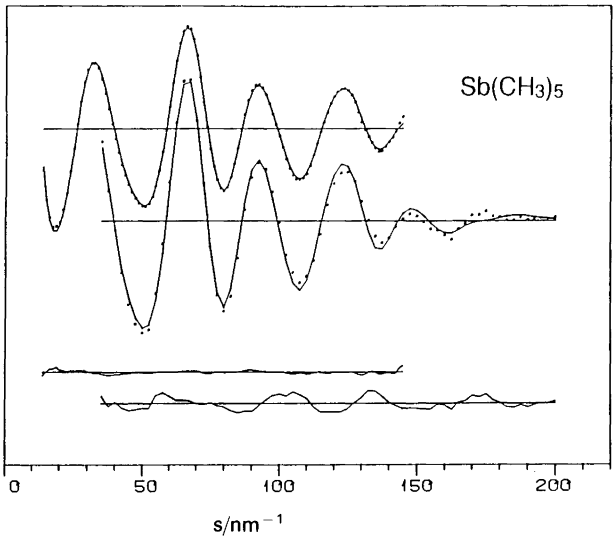

Fig. 1. Calculated (full line) and experimental (·) modified molecular intensity curves for $Sb(CH_3)_5$ with difference curves below.

Calculations

Normal coordinate analysis. Calculations were based on the molecular model shown in Fig. 2. The SbC_5 frame was assumed to have D_{3h} symmetry, and methyl groups were assumed to be isostructural and to have C_{3v} symmetry with the symmetry axes along the Sb–C bonds; the orientations are indicated in the figure. A symmetry force field was constructed from the valence force field of the SbC_5

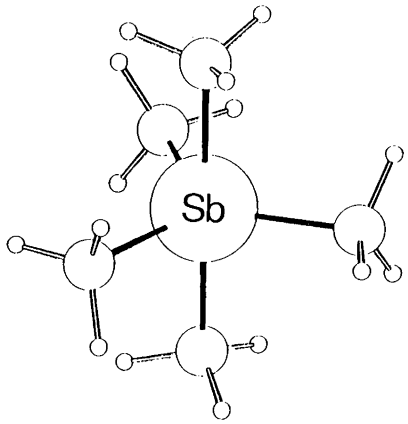

Fig. 2. Molecular model of $Sb(CH_3)_5$ with trigonal bipyramidal configuration. The molecular symmetry (equatorial H atoms excluded) is D_{3h}.

frame listed in Ref. 22 and the force constants of the methyl groups in $(CH_3)_4Sn_4S_6$.[23] Root-mean-square vibrational amplitudes, *l*, and the vibrational correction parameters, $D_{ij} = r_{\alpha ij} - r_{aij}$, calculated from this symmetry force field, are listed in Table 1.[24]

Structure refinement. The molecular model in Fig. 2 is described by four independent parameters, e.g. the bond distances Sb–C_{ax}, Sb–C_{eq} and C–H and the valence angle ∠ Sb–C–H. These structure parameters and ten vibrational amplitudes were refined by least-squares calculations on the molecular intensity curves under the constraints of a geometrically consistent r_α-structure. Non-refined amplitudes were fixed at the values calculated from the molecular force field. The refinements converged to the best values listed in Table 1. Since the refinements were carried out with a diagonal weight matrix, the estimated standard deviations listed in the table have been multiplied by a factor of 3.0 to include the uncertainty induced by data correlation[25] and non-refined amplitudes, and then expanded to include an estimated scale uncertainty of 0.1%. The molecular intensities calculated for the best model are good agreement with the experimental intensities obtained from the 50 cm plates (Fig. 1). The difference between calculated intensities and the experimental counterparts obtained from 25 cm plates is of the order expected from the noise level of the latter.

Table 1. Interatomic distances, r_a, root-mean-square vibrational amplitudes, *l*, obtained by gas electron diffraction (ED), and vibrational amplitudes and vibrational correction terms, *D*, calculated from a molecular symmetry force field (FF). When appropriate, distance multiplicities ($n_{ij}\times$) are indicated in parentheses. Non-refined parameters are in square brackets.

	r_a(ED)/ pm	*l*(ED)/ pm	*l*(FF)/ pm	*D*(FF)/ pm
Bond distances				
Sb–C_{eq}	214.0(5)	[5.4]	5.4	−0.3
Sb–C_{ax}	226.4(11)	[6.1]	6.1	−0.8
C_{eq}–H (3×)	110.4(6)[a]	10.3(7)[b]	7.8	−6.5
C_{eq}–H (6×)	110.4(6)[a]	10.3(7)[b]	7.8	−7.1
C_{ax}–H	110.4(6)[a]	10.3(7)[b]	7.8	−3.1
Nonbonded distances				
Sb–H_{eq} (3×)	271(3)	13.4(15)[c]	12.6	−2.3
Sb–H_{eq} (6×)	271(3)	13.4(15)[c]	12.6	−2.9
Sb–H_{ax}	282(4)	13.7(15)[c]	12.9	−1.7
C_{ax}–C_{eq}	310.9(7)	11.3(18)	14.5	−0.2
C_{eq}–C_{eq}	370.0(9)	23(10)	10.6	0.0
C_{ax}–C_{ax}	451.3(22)	12(9)	8.5	0.0
C_{ax}–H_{eq}	292(4)	16(20)[d]	27.6	−0.7
C_{ax}–H_{eq}	351(3)	27(20)[d]	28.5	0.3
C_{ax}–H_{eq}	404(2)	17(7)[e]	19.5	−1.6
C_{eq}–H_{ax} (12×)	321(4)	34(26)	23.7	0.0
C_{eq}–H_{ax} (6×)	409(2)	14(7)[e]	15.5	−1.1
C_{eq}–H_{eq} (3×)	369(3)	[19.4]	19.4	−1.1
C_{eq}–H_{eq} (6×)	392(3)	30(46)	22.5	−0.7
C_{eq}–H_{eq} (6×)	436(2)	[15.0]	20.5	−0.9
C_{eq}–H_{eq} (3×)	457(2)	[13.1]	13.1	−1.5
C_{ax}–H_{ax}	498(5)	14(9)	16.1	−0.3
Valence angles				
∠αSb–C–H/°	110.5(22)[a]			
∠αC_{eq}–Sb–C_{eq}/°	[120]			
∠αC_{ax}–Sb–C_{eq}/°	[90]			
R-factors[f]	0.032 (50 cm)	0.116 (25 cm)	0.057 (total)	

[a] Mean value. [b] Assumed equal. [c–e] Refined with constant differences. [f] $R = \{[\sum w (I_{obs} - I_{calc})^2]/[\sum w I_{obs}^2]\}^{1/2}$.

Table 2. Structure parameters obtained by optimizing D_{3h} and C_{4v} models of $Sb(CH_3)_5$ at all-electron SCF level and of $Bi(CH_3)_5$ at SCF/ECP level.

	Trigonal bipyramid		Square pyramid		
	M–C_{ax}/ pm	M–C_{eq}/ pm	M–C_{ap}/ pm	M–C_b/ pm	∠ $C_{ap}MC_{ba}$/°
Sb–C	224	219	216	223	103
[exp]	[226][a]	[214][a]	[212][b]	[225][b]	[102][b]
Bi–C	232	231	229	232	102
[exp]	[239][c]	[218][c]	[221][d]	[233][d]	[102][d]

[a] This work. [b] $SbPh_5$(cr).[3]
[c] $Bi(m\text{-}C_6H_4Me)_3(o\text{-}C_6H_4F)^2$(cr).[13] [d] $BiPh_5$(cr).[4]

A square pyramidal model with a SbC_5 framework of C_{4v} symmetry is described by an apical Sb–C bond distance, four identical basal Sb–C bond distances, the valence angle ∠ C_{ap}–Sb–C_{ba} and the mean C–H bond distance and ∠ Sb–C–H valence angle. Exploratory least-squares refinements on this model yielded *R*-factors above 0.12 as compared with 0.057 for the best model, and failed to converge. When refinements were carried out on models of C_{2v} symmetry, calculations with start parameters corresponding to near-C_{4v} symmetry converged to models of near-D_{3h} symmetry. We conclude that models of C_{4v} symmetry are incompatible with the gas electron diffraction data.

SCF molecular orbital calculations. All SCF calculations were performed with the MOLECULE SWEDEN program package.[26]

Table 3. Electronic energy, Δ*E*, of $M(CH_3)_5$, M = Sb or Bi, in the square pyramidal, C_{4v}, configuration relative to the more stable trigonal bipyramidal, D_{3h}, configuration.

	Δ*E*/kJ mol
$Sb(CH_3)_5$	
SCF	12.1
SCF/ECP	11.3
SCF/ECP/MCPF	7.1
$Bi(CH_3)_5$	
SCF/ECP	13.4
SCF/ECP/MCPF	10.5

For Sb we used an all-electron basis set of (15,11,8) primitive Gaussians[27] supplemented by two diffuse d-functions with exponents 0.20 and 0.05 representing the 5d orbitals, contracted to ⟨6,5,3⟩. For C and H we used a (7,3) basis[28] contracted to ⟨3,2⟩ and a (3) basis[29] contracted to ⟨2⟩, respectively.

The C–H bond distances and ∠Sb–C–H angles were fixed at the electron diffraction values, and the axial and equatorial Sb–C bond distances of a trigonal bipyramidal model (Fig. 2) optimized at the HF level. The optimal bond distances are listed in Table 2. Similar optimization of the apical and basal Sb–C bond distances and the valence angle $\angle C_{ap}$–Sb–C_{ba} for a square pyramidal model yielded an optimal energy which was $\Delta E =$ 12.1 kJ mol^{-1} higher. The optimal structure parameters are listed in Table 2. Unfortunately our computational resources did not allow dermination of the molecular force field.

Relativistic effects were included by the use of relativistic effective core potentials (RECP) based on relativistic no-pair atomic calculations.[30] The method is described in Ref. 31 and references therein. The valence shell ($n = 5$) and the sub-valence shell ($n = 4$) orbitals were described by a primitive (7,6,6) basis contracted to ⟨3,3,3⟩. Three of these contracted orbitals represent the 4s, 4p and 4d orbitals, respectively; the 5s, 5p and 5d orbitals were described at the double-zeta level.

The energy difference between C_{4v} and D_{3h} configurations was obtained by one-point SCF ECP calculations on the two optimal models (Table 3). Finally, electron correlation was included by calculations with the modified coupled pair functional (MCPF) method.[32] This method is size-consistent, and it was possible to correlate all 40 valence electrons.

The large number of electrons precluded all-electron calculations on $Bi(CH_3)_5$, and only RECP calculations were carried out. The atomic reference calculations were carried out with a (19,16,8,5) primitive basis.[33] The RECP calculations were carried out with the 6s, 6p and 6d orbitals described at the double-zeta and the 5s, 5p, 5d and 4f orbitals at the single-zeta level by a primitive (7,6,6,1) basis contracted to ⟨3,3,3,1⟩. Optimization of D_{3h} and C_{4v} models yielded the structure parameters listed in Table 2 and the energy differences listed in Table 3. Finally, electron correlation was estimated by MCPF calculations on all valence electrons.

Results and discussion

While attempts to record GED data for $Sb(CH_3)_5$ with an inlet system made from metal have been unsuccessful owing to partial decomposition of the sample, experiments with an all-glass inlet system proceeded without difficulty. The data thus obtained are incompatible with molecular models of C_{4v} or near C_{4v} symmetry, and in good agreement with trigonal bipyramidal models where the SbC_5 frame has D_{3h} symmetry. Our investigation thus confirms the conclusion reached in the earlier investigation by vibrational spectroscopy.[16]

Table 4. Axial and equatorial bond distances in some trigonal bipyramidal Sb(V) compounds.

Compound	Sb–C_{ax}/pm	Sb–C_{eq}/pm	Ref.
$Sb(CH_3)_5$(g)	226.4(10)	214.0(8)	This work
$SbPh_5$ 1/2 (c-C_6H_{12})(cr)	224	214	5
$Sb(CCCH_3)_5$(cr)	215	206	34
$Sb(CCCH_3)_2(CH_3)_3$(cr)	223[a]	214[b]	35
	Sb–X_{ax}		
$SbCl_2(CH_3)_3$(g)	246.0(6)	210.7(6)	36
$SbF_2(CH_3)_3$(cr)	200	209	37
		Sb–Cl_{eq}	
$SbCl_5$(g)	233.8(7)	227.7(5)	38

[a] Propynyl. [b] Methyl.

In Table 4 we compare axial and equatorial Sb–C bond distances with bond distances in related Sb(V) compounds. The observed variation of axial and equatorial bond distances, axial Sb–C from 226 to 215 pm, equatorial Sb–C from 214 to 206 pm, may be discussed in terms of a bonding radius of C, which depends on the hybridization, and in terms of a bonding radius of Sb, which depends on the number of electronegative substituents. The bond distances in the table indicate that the former effect is less important than the latter. The three equatorial Sb–C bonds in $Sb(CH_3)_5$, in $SbPh_5$ crystallized with 0.5 mol of cyclohexane or in dipropynyl(trimethyl)antimony are indistinguishable. The axial Sb–C bonds in $SbPh_5$ 1/2(c-C_6H_{12}) and dipropynyl(trimethyl)antimony are only 2–3 pm shorter than in $Sb(CH_3)_5$. If the difference is real, it may be

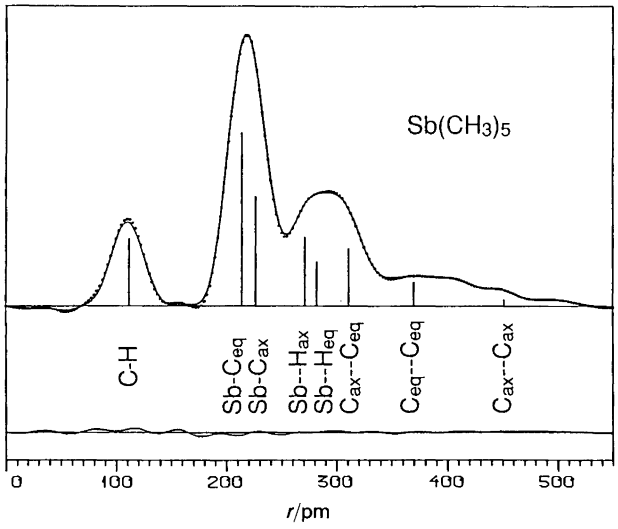

Fig. 3. Calculated (full line) and experimental (·) radial distribution curves for $Sb(CH_3)_5$. The artificial damping constant $k = 30$ pm^2. The most important peaks are indicated by bars of height approximately equal to the weight of the distance in the theoretical intensity curve. The difference curve is shown below.

rationalized by assuming that the bonding radii of sp^2 or sp hybridized C are smaller than the bonding radius of sp^3 hybridized.

When two methyl groups in $Sb(CH_3)_5$ are replaced by more electronegative groups such as propynyl, or by Cl or F atoms, these occupy axial positions as expected. Introduction of two axial propinyl groups does not seem to affect the equatorial Sb–C bond distances, but introduction of two axial halogen atoms leads to progressive shortening of equatorial Sb–C bond distances from 214 pm in $Sb(CH_3)_5$ to 211 pm in $SbCl_2(CH_3)_3$ and 209 pm in $SbF_2(CH_3)_3$.

Finally we consider the effect of electronegative substituents in equatorial positions on axial bond distances. Replacement of the three equatorial methyl groups in $SbCl_2(CH_3)_3$ by three Cl atoms shortens the axial Sb–Cl bonds from 246 to 234 pm, and introduction of three equatorial propenyl groups in $Sb(CCCH_3)_2(CH_3)_3$ shortens the axial Sb–C (propynyl) bonds from 223 to 215 pm.

We conclude that the axial bonds are more sensitive to substitution in the equatorial position than vice versa.

^{13}C-NMR spectra of $Sb(CH_3)_5$ in CD_2Cl_2 contained only one peak, which became sharper with decreasing temperature to −90°C. The inverse line-broadening is probably due to quadrupole effects. The spectra thus provide no information on the barrier to exchange of axial and equatorial methyl groups, except that it must be small.

Optimization of a molecular model of $Sb(CH_3)_5$ of D_{3h} symmetry by all-electron SCF calculations yielded axial and equatorial Sb–C bond distances that were 2 pm shorter and 5 pm longer than the experimental values. Optimization of a square pyramidal, C_{4v} model yielded apical and basal Sb–C bond distances and a valence angle $\angle C_{ap}$–Sb–C_{ba} close to the mean values in crystalline $SbPh_5$ (Table 2). The trigonal bipyramidal configuration was calculated to be more stable than the square pyramidal by 12.1 kJ mol^{-1} at the all-electron SCF level and 7.1 kJ mol^{-1} at the relativistic ECP/MCPF level. The latter energy is very similar to the observed barrier to exchange of ligands in pentatolylantimony, about 6.4 kJ mol^{-1}.[9]

Some Mulliken population parameters are listed in Table 5. The gross atomic populations suggest that the net atomic charge on the metal atom in $Sb(CH_3)_5$ in the equilibrium configuration is about +0.8 at the highest computational level (MCPF), and that the negative charge on the axial methyl groups is greater than the negative charge on the equatorial. The charge distribution is thus consistent with the known predilection for the more electronegative substituent to occupy axial positions.

. The total 5d orbital population, defined as the total orbital population minus 20, is 0.68 at the highest computational level, while the $5d_{z^2}$ population, defined as the total d_{z^2} population minus 4, is 0.43. Thus the $5d_{z^2}$ orbital population is about two thirds of the total hypervalent 5d orbital population.

The three equatorial Sb–C bonds in $Sb(CH_3)_5$ may be described in terms of two-center two-electron bonds formed from sp^2 hybrids on Sb. Bonding between Sb and the two axial C atoms may be described in terms of two-center two-electron bonds formed from two $p_z d_{z^2}$ hybrids on Sb, or in terms of a three-center four electron system involving the $5p_z$ orbital only.[39] The first description implies a $5d_{z^2}$ population of about one electron, the second that the $5d_{z^2}$ orbital remains unoccupied. For what they are worth, the population parameters suggest that the description in terms of a three-center four-electron system may be the more appropriate, though the role of the $5d_{z^2}$ orbital is not negligible.

We had hoped that the calculations on the square pyramidal model should yield higher hypervalent *d* orbital populations than calculations on the trigonal prismatic model, thus providing support for our proposal that the square pyramidal structure observed for $Ta(CH_3)_5$ is due to greater d orbital contributions to the bonding.[40] This hope was, however, not fulfilled.

$Bi(CH_3)_5$ appears to be unknown. Since the stability of the square pyramidal configuration relative to the trigonal bipyramidal increases from PPh_5 to $BiPh_5$, we nevertheless thought it worth while to carry out optimization of the two structures at the ECP level and to calculate the energy difference at the ECP/MCPF level. The difference between the calculated bond distances and the

Table 5. Mulliken population parameters for $M(CH_3)_5$ M = Sb or Bi, with molecular symmetries = D_{3h} or C_{4v} obtained at different computational levels. Me = CH_3.

Central atom, M	Sb	Sb	Sb	Sb	Sb	Sb	Bi	Bi	Bi	Bi
Point group	D_{3h}	D_{3h}	D_{3h}	C_{4v}	C_{4v}	C_{4v}	D_{3h}	D_{3h}	C_{4v}	C_{4v}
Computational level	AE-SCF	ECP-SCF	MCPF	AE-SCF	ECP-SCF	MCPF	ECP-SCF	MCPF	ECP-SCF	MCPF
Total hypervalent d orbital population (5d for Cd, 6d for Bi)	0.62	0.63	0.68	0.62	0.63	0.68	0.91	0.95	0.92	0.97
Hypervalent d_{z^2} orbital population for D_{3h}; $d_{x^2-y^2}$ population for C_{4v}	0.32	0.45	0.43	0.32	0.36	0.33	0.65	0.63	0.54	0.52
Net charge: Sb viz. Bi	+1.41	+1.17	+0.83	+1.42	+1.05	+0.71	+1.42	+1.08	+1.47	+1.12
Net charge: Me_{ax} viz. Me_{ap}	−0.34	−0.30	−0.21	−0.25	−0.16	−0.10	−0.33	−0.26	−0.27	−0.20
Net charge: Me_{eq} viz. Me_{ba}	−0.25	−0.19	−0.13	−0.29	−0.22	−0.15	−0.25	−0.19	−0.30	−0.23

bond distances found in crystalline substituted pentaphenyls is larger than for $Sb(CH_3)_5$ (Table 2). The energy of the square pyramidal configuration is calculated to be 10.5 kJ mol^{-1} above the energy of the trigonal bipyramidal. Thus our calculations suggest that the equilibrium configuration of $Bi(CH_3)_5$ would be trigonal bipyramidal like $Sb(CH_3)_5$.

Acknowledgments. We are grateful to the Norwegian Research Council of Science and the Humanities (NAVF) and to the VISTA Program of Statoil and the Norwegian Academy of Science and Letters for financial support.

References

1. Wheatley, P. J. and Wittig, G. *Proc. Chem. Soc. London* (1962) 251.
2. Wheatley, P. J. *J. Chem. Soc.* (1964) 2206.
3. Wheatley, P. J. *J. Chem. Soc.* (1964) 3718; Beauchamps, A. L., Bennet, M. J. and Cotton, F. A. *J. Am. Chem. Soc. 51* (1973) 6675.
4. Schmuck, A., Buschmann, J., Fuchs, J. and Seppelt, K. *Angew. Chem. 99* (1987) 1206; *Angew. Chem., Int. Ed. Engl. 26* (1987) 1180.
5. Brabant, C., Blanck, B. and Beauchamp, A. L. *J. Organomet. Chem. 82* (1974) 231.
6. Brabant, C., Hubert, J. and Beauchamp, A. L. *Can. J. Chem. 51* (1973) 2951.
7. Beattie, R., Livington, K. M. S., Ozin, G. A. and Sabine, R. *J. Chem. Soc., Dalton Trans.* (1972) 784.
8. Berry, R. *J. Chem. Phys. 32* (1960) 933.
9. Kuykendall, G. L. and Mills, J. L. *J. Organometal. Chem. 118* (1976) 123.
10. Schmuck, A., Buschmann, J., Fuchs, J. and Seppelt, K. *Angew. Chem. 99* (1987) 1208.
11. Schmuck, A. and Seppelt, K., *Chem. Ber. 122* (1989) 803.
12. Schmuck, A., Leopold, D., Wallenhauer, S. and Seppelt, K. *Chem. Ber. 123* (1990) 761.
13. Schmuck, A., Pyykkö, P. and Seppelt, K. *Angew. Chem. 102* (1990) 211.
14. Wittig, G. and Torsell, K. *Acta Chem. Scand. 7* (1953) 1293.
15. Mitschke, K.-H. and Schmidbaur, H. *Chem. Ber. 106* (1973) 3645.
16. Downs, A. J., Schmutzler, R. and Steer, I. A. *Chem. Commun.* (1966) 221.
17. Muetterties, E. L., Mahler, W., Packer, K. J. and Schmutzler, R. *Inorg. Chem. 3* (1964) 1298.
18. Goel, R. G., Maslowsky, E., Jr. and Senoff, C. V. *Inorg. Chem. 10* (1971) 2527 and references therein.
19. Bastiansen, O., Graber, R. and Wegmann, L. *Balzers High Vac. Rep. 25* (1969) 1.
20. Andersen, B., Seip, H. M., Strand, T. G. and Stølevik, R. *Acta Chem. Scand. 23* (1969) 3224.
21. Schäfer, L., Yates, A. C. and Bonham, R. A. *J. Chem. Phys. 55* (1971) 3055; *International Tables for X-Ray Crystallography*, Kynoch Press, Birmingham 1974, Vol. 4.
22. Nevett, B. A. and Perry, A. *J. Mol. Spectrosc. 66* (1977) 331.
23. Müller, A., Nolte, W., Cyvin, S. J., Cyvin, B. N. and Alix, A. J. P. *Spectrochim. Acta, Part A 34* (1978) 383.
24. Kuchitsu, K. and Cyvin, S. J. In Cyvin, S. J., Ed., *Molecular Structures and Vibrations*, Elsevier, Amsterdam 1972.
25. Seip, H. M., Strand, T. G. and Stølevik, R. *Chem. Phys. Lett. 3* (1969) 617.
26. MOLECULE is a vectorized Gaussian integral program written by J. Almlöf. SWEDEN is a vectorized SCF-CASSCF, direct CI and CCI program written by P. Siegbahn, B. Roos, P. Taylor, A. Heiberg, J. Almlöf, S. R. Langhoff and D. P. Chong.
27. Strömberg, A., Gropen, O. and Wahlgren, U. *J. Comput. Chem. 4* (1983) 181.
28. van Duijnevelt, F. B. *IBM Technical Report No. RJ-945* (1971).
29. Huzinaga, S. *J. Chem. Phys. 42* (1965) 1293.
30. Almlöf, J., Fægri, K., and Grelland, H. *Chem. Phys. Lett. 114* (1985) 53.
31. Gropen, O. In Wilson, S., Ed., *Methods in Computational Chemistry*, Plenum, New York 1988.
32. Chong, D. P. and Langhoff, S. R. *J. Chem. Phys. 84* (1986) 5606.
33. Gropen, O. *J. Comput. Chem. 8* (1987) 982.
34. Tempel, N., Schwarz, W. and Weidlein, J. *Z. Anorg. Allg. Chem. 474* (1981) 157.
35. Tempel, N., Schwarz, W. and Weidlein, J. *J. Organomet. Chem. 154* (1978) 21.
36. Shen, Q. and Hemmings, R. T. *J. Mol. Struct. 197* (1989) 349.
37. Schwarz, W. and Guder, H. J. *Z. Anorg. Allg. Chem. 444* (1978) 105.
38. Ivashkevich, L. S., Ishchenko, A. A., Spiridonov, V. P., Strand, T. G., Ivanov, A. A. and Nikolaev, A. N. *J. Struct. Chem. USSR 23* (1982) 295.
39. Musher, J. I. *Angew. Chem. 81* (1969) 68.
40. Pulham, C., Haaland, A., Hammel, A., Rypdal, K., Verne, H. P. and Volden, H. V. *Angew. Chem. 104* (1992) 1534.

Received August 23, 1992.